

STM Physical Backgrounds

Tunneling Effect

The idea of particles tunneling appeared almost simultaneously with quantum mechanics. In **classical mechanics**, to describe a system of material points at a certain moment of time, it is enough to set every point coordinates and momentum components. In **quantum mechanics** it is in principle impossible to determine simultaneously coordinates and momentum components of even single point according to the Heisenberg uncertainty principle. To describe the system completely, an associated complex function is introduced in quantum mechanics (**the wavefunction**). The wavefunction Ψ , which is a function of time and all system particles position, is a solution of the wave Schrodinger equation. In order to use the system wavefunction, one should determine $|\Psi|^2$ rather than Ψ . Then, the probability for finding particles in an elementary volume $dxdydz$ is given by $|\Psi|^2 dxdydz$.

If particles impinge on a potential barrier of a limited width, the quantum mechanics predicts the effect of particles penetration through the potential barrier even if particle total energy is less than the barrier height which is unknown in classical physics.

Lets calculate the transparency of the rectangular barrier [1], [2]. Suppose that electrons of potential energy

$$U(z) = \begin{cases} 0, & \text{npu } z < 0; \\ U_0 & \text{npu } 0 \leq z \leq L; \\ 0, & \text{npu } z > L \end{cases} \quad (1)$$

impinge on the rectangular potential barrier and the total energy E is less than U_0 (Fig. 1).

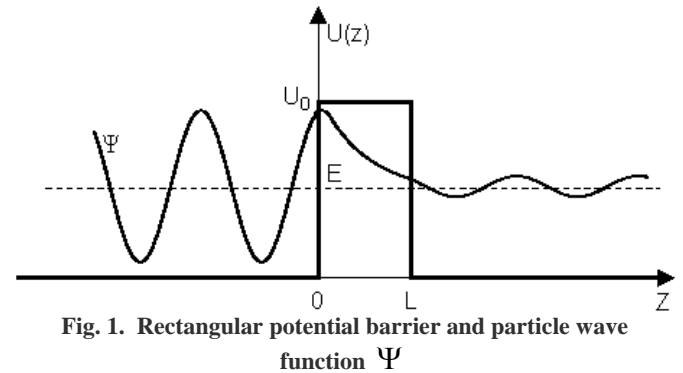


Fig. 1. Rectangular potential barrier and particle wave function Ψ

The stationary Schrodinger equations can be written as follows

$$\begin{cases} \ddot{\Psi} + \kappa_1^2 \Psi = 0, & \text{npu } z < 0; \\ \ddot{\Psi} - \kappa_2^2 \Psi = 0, & \text{npu } z \in [0; L]; \\ \ddot{\Psi} + \kappa_1^2 \Psi = 0, & \text{npu } z > L \end{cases} \quad (2)$$

where $\kappa_1 = \frac{\sqrt{2mE}}{\hbar}$, $\kappa_2 = \frac{\sqrt{2m(U_0 - E)}}{\hbar}$ – wave vectors, $\hbar = 1,05 \cdot 10^{-34} \text{ Дж} \cdot \text{с}$ – Planck's constant. The solution to the wave equation at $z < 0$ can be expressed as a sum of incident and reflected waves $\Psi = \exp(ik_1 z) + a \exp(-ik_1 z)$, while solution at $z > L$ – as a transmitted wave $\Psi = b \exp(ik_1 z)$. A general solution inside the potential barrier $0 < z < L$ is written as $\Psi = c \exp(k_2 z) + d \exp(-k_2 z)$. Constants a , b , c , d are determined from the wavefunction Ψ and $\dot{\Psi}$ continuity condition at $z=0$ and $z=L$.

The barrier transmission coefficient can be naturally considered as a ratio of the transmitted electrons probability flux density to that one of the incident electrons. In the case under consideration this ratio

is just equal to the squared wavefunction module at $z > L$ because the incident wave amplitude is assumed to be 1 and wave vectors of both incident and transmitted waves coincide.

$$D = bb^* = \left(ch^2(k_2 L) + \frac{1}{4} \left(\frac{k_2}{k_1} - \frac{k_1}{k_2} \right)^2 sh^2(k_2 L) \right)^{-1} \quad (3)$$

If $k_2 L \gg 1$, then both $ch(k_2 L)$ and $sh(k_2 L)$ can be approximated to $\exp(k_2 L)/2$ and (3) will be written as

$$D(E) = D_0 \exp \left\{ -\frac{2L}{\hbar} \sqrt{2m(U_0 - E)} \right\} \quad (4)$$

where
$$D_0 = 4 \left[1 + \frac{1}{4} \left(\frac{k_2}{k_1} - \frac{k_1}{k_2} \right)^2 \right]^{-1}.$$

Thus, analytical calculation of the rectangular barrier transmission coefficient is rather a simple task. However, in many quantum mechanical problems it is necessary to find the transmission coefficient of the more complicated shape barrier. In this case, there is no common analytical solution for the D coefficient. Nevertheless, if the problem parameters satisfy the quasiclassical condition, the transmission coefficient can be calculated in a general form. (see chapter [Tunneling Effect in Quasiclassical Approximation](#)).

Summary

- In quantum mechanics tunneling effect is particles penetration through the potential barrier even if particle total energy is less than the barrier height.
- To calculate the transparency of the potential barrier, one should solve Shrodinger equation at continuity condition of wavefunction and its first derivative.
- The transparency coefficient of the rectangular barrier decreases exponentially with the barrier width, when wave vectors of both incident and transmitted waves coincide.

References

1. Sivuhin D.V. A General course of physics. Nauka, volume 5, chapter 1, 1988 (In Russian)
2. Goldin L.L., Novikova H.I. The introduction in quantum physics. Nauka, 1988 (In Russian).

Tunneling Effect in Quasiclassical Approximation

The quasiclassical qualitative condition imply that de Broglie wavelength of the particle λ is less than characteristic length L determining the conditions of the problem. This condition means that the particle wavelength should not change considerably within the length of the wavelength order

$$\left| \frac{d\tilde{\lambda}}{dz} \right| \ll 1 \quad (1)$$

where $\tilde{\lambda} = \lambda / 2\pi$, $\lambda(z) = 2\pi\hbar / p(z)$ – de Broglie wavelength of the particle expressed by way of the particle classical momentum $p(z)$ [1].

Condition (1) can be expressed in another form taking into account that

$$\frac{dp}{dz} = \frac{d}{dz} \sqrt{2m(W - U)} = -\frac{m}{p} \frac{dU}{dz} = \frac{mF}{p} \quad (2)$$

where $F = -dU/dz$ means classical force acting upon the particle in the external field.

Introducing this force, we get

$$\frac{m\hbar|F|}{p^3} \ll 1 \quad (3)$$

From (3) it is clear that the quasiclassical approximation is not valid at too small momentum of the particle. In particular, it is deliberately invalid near positions in which the particle, according to classical mechanics, should stop, then start moving in the opposite direction. These points are the so called "turning points". Their coordinates z_1 and z_2 are determined from the condition $E = U(z)$.

It should be emphasized that condition (3) itself can be insufficient for the permissibility of the quasiclassical approach. One more condition should be met: the barrier height should not change much over the length L .

Let us consider the particles move in the field shown in Fig. 1 which is characterized by the presence of the potential barrier with potential energy $U(z)$ exceeding particle total energy E and meeting all the quasiclassics conditions. In this case points z_1 and z_2 are the turning points.

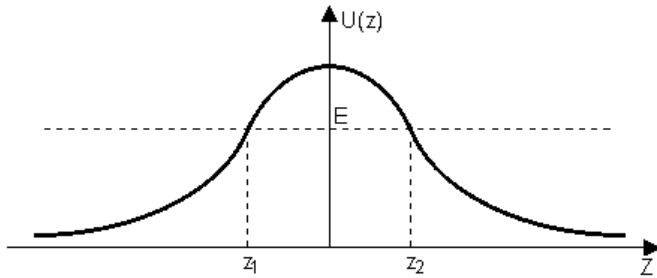


Fig. 1. Potential barrier of arbitrary shape

The approximation technique of the Schrodinger equation solution when quasiclassical conditions are met was first used by Wentzel, Kramers and Brillouin. This technique is known as WKB approximation or quasiclassical quantization method. In this textbook we do not present the Schrodinger equations solution for the given case. However, it can be found in [1], [2] and the barrier transparency in this case is

$$D(E) \propto \exp \left\{ -\frac{2}{\hbar} \int_{z_1}^{z_2} \sqrt{2m(U(z) - E)} dz \right\} \quad (4)$$

Comparing expressions (3) in chapter [Tunneling Effect](#) for transmission coefficients of rectangular barrier (precise solution of Shrodinger equation) and (4) for quasiclassical approximation, we can notice that there is no qualitative difference between them. In both cases the transparency decreases exponentially with the barrier width.

Summary

- If the problem parameters satisfy quasiclassical conditions, then transmission coefficient can be calculated in a general form using (4).
- In case of the square barrier there is no qualitative difference between transmission coefficients calculated using quantum mechanics and quasiclassical approximation. In both cases the transparency decreases exponentially with the barrier width.

References

1. Landau L.D., Lifshitz E. M. Quantum mechanics. Nauka, 1989 (In Russian)
2. Mott N., Sneddon I. Wave mechanics and its application. Nauka, 1966 (In Russian)

Metal Energy-Band Structure

To derive the formula of tunneling current in the metal-insulator-metal (MIM) system (John G. Simmons formula, see [chapter "John G. Simmons Formula"](#)), we must make some assumptions and remind of metal electronic theory fundamentals.

- Firstly, let us consider that the solid (metal) is a three-dimensional potential well with a plain bottom (the so called Sommerfeld model) and electrons do not interact with each other. The energy of the electron resting at the bottom of such potential well is less than vacuum level – the energy of electron resting infinitely far from the solid surface. The well depth U is determined by the averaged field of all positive ions of the lattice and of all electrons.
- Secondly, because all electrons are considered to be noninteracting, the solution to the Schrodinger equation for the system of electrons is turned to the solution to the Schrodinger equation for single electron moving in the averaged field which allows to use formulas (3) in chapter [Tunneling Effect](#) or (4) in chapter [Tunneling Effect in Quasiclassical Approximation](#).
- Thirdly, in the potential box with the plain bottom, the dependence of energy allowed values on wave vector allowed values looks like points on the parabolic dependence of the energy on the wave vector components $E = p^2 / 2m = (\hbar k)^2 / 2m$ for the free electron in void. If electrons mass m is isotropic in space, then the following expression is valid $E = p_x^2 / 2m + p_y^2 / 2m + p_z^2 / 2m = p^2 / 2m$, where P_x, P_y, P_z – axial electron momentum components.

From the statistical physics [1] it is known that in a system in thermodynamic equilibrium all quantum states with the same energy level E are occupied with electrons equally. The mean number of electrons in one quantum state with energy E at

temperature T is given by the Fermi-Dirac distribution:

$$f(E) = \frac{1}{1 + \exp\left(\frac{E - \mu}{k_B T}\right)} \quad (1)$$

where $k_B = (11600)^{-1}$ eV/K – Boltzmann's constant, μ – parameter having the dimension of energy and called chemical potential.

The chemical potential μ is defined by the normalization condition

$$\int_0^\infty n(E) f(E) dE = n_e \quad (2)$$

where n_e – number of conduction band electrons per volume unit (concentration),

$$n(E) dE = 2(2\pi)^3 \iiint_{[E, E+dE]} d^3k = \frac{1}{2\pi^2} \left(\frac{\sqrt{2m}}{\hbar} \right)^3 \sqrt{E} dE -$$

number of electron states per volume unit in the energy range from E to $E + dE$. $n(E)$ function is called the energetic density of states.

In a metal at the temperature close to absolute zero, electrons occupy all quantum states with energies up to the level $\mu_0 = \mu(0)$ called the Fermi level. All quantum states above the Fermi level are not occupied with electrons. In a metal, the chemical potential slightly depends on temperature, therefore it can be approximated by μ_0 at $T = 0$:

$$\mu(T) \approx \mu_0 = \frac{\hbar^2}{2m} (3\pi^2 n_e)^{2/3} \quad (3)$$

where m – electron mass. If n_e is expressed in C.G.S. units, then $\mu_0 = 0,36 \cdot 10^{-14} n_e^{2/3} \text{ eV}$.

If a system is in thermal equilibrium and consists of some sub-systems, the Fermi levels of subsystems should be the same (Fig. 1). If voltage V is applied between two subsystems (solids), the Fermi level of the solid connected to the positive pole decreases, while for the other solid it increases. The difference in Fermi levels between solids is eV (Fig. 2).

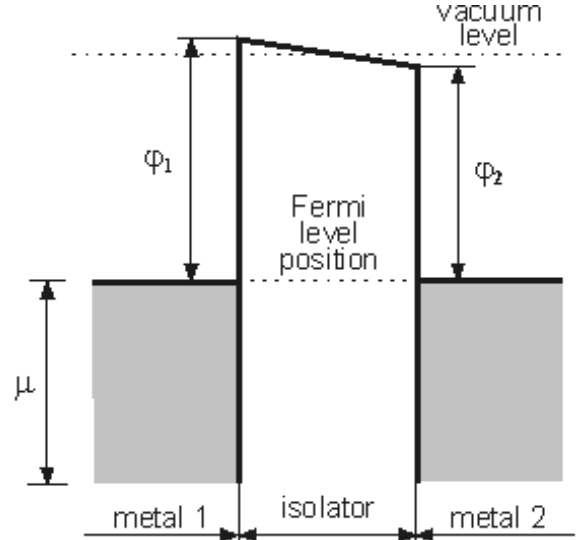


Fig. 1. Diagram of MIM system in equilibrium.
 j_1 and j_2 – work function of the left and right metals, respectively

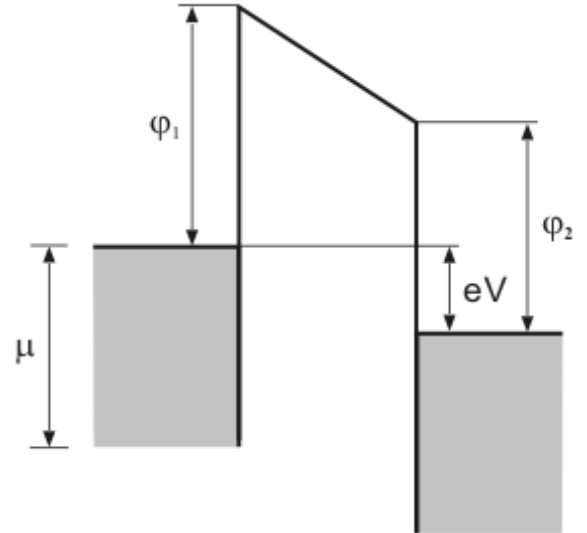


Fig. 2. Model of MIM system then positive potential is applied to the right metal

Summary

To derive the formula of tunneling current in the MIM system ([chapter "John G. Simmons Formula"](#)) we assume that:

- Sommerfeld model is correct for all solid bodies.
- Each electron from the solid move in averaged field of all positive ions of the lattice and of all electrons.
- Isotropic square-law of dispersion as for free electron in void is correct (1).
- In a metal at $T \rightarrow 0K$, electrons occupy all quantum states with energies up to the Fermi level μ_0 (3). All quantum states above the Fermi level are not occupied with electrons.

References

1. Landau L.D., Lifshitz E. M. Statistical physics. Nauka, 1976 (in Russian)
2. Kittel Ch. Introduction in solid-state physics. Nauka, 1978 (in Russian)

CONTACT DETAILS

Building 167, Zelenograd, 124460, Moscow, Russia
Tel: +7(095)535-0305, 913-5736
Fax: +7(095) 535-6410, 913-5739

e-mail: spm@ntmdt.ru; <http://www.ntmdt.ru>

Tunnel Current in MIM System

John G. Simmons Formula

Now, using the Sommerfeld model (see [chapter "Metal Energy-Band Structure"](#)) and WKB approximation (see [chapter "Tunneling Effect in Quasiclassical Approximation"](#)) and assuming that $T = 0$, potential barrier is of arbitrary shape and the mass of electrons is isotropic in space, we can derive an expression for the tunneling current flowing in a metal-insulator-metal (MIM) system.

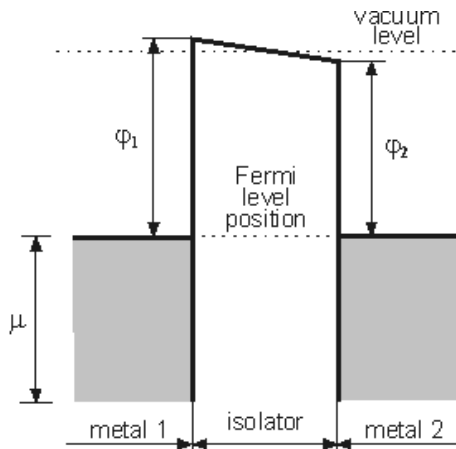


Fig. 1. Diagram of MIM system in equilibrium.
j1 and j2 – work function of the left and right metals, respectively

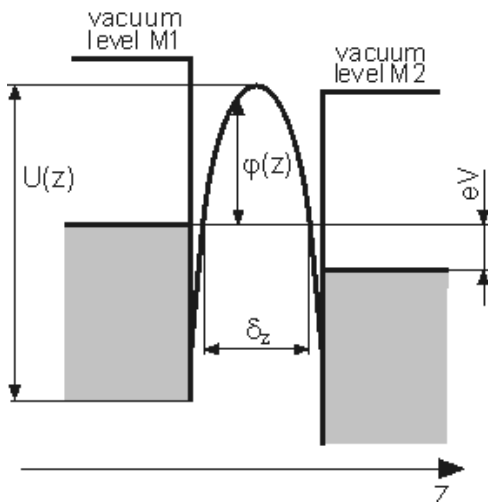


Fig. 2. Model of MIM system with an arbitrary shape potential barrier. Positive potential is applied to the right metal

Consider two metal electrodes with an insulator of thickness L between them. If electrodes are under the same potential, the system is in thermodynamic equilibrium (see [chapter "Metal Energy-Band Structure"](#)) and Fermi levels of electrodes coincide (Fig. 1). However, if electrodes are under different potentials, current flow between them is available. Fig. 2 shows the energy diagram of electrodes with applied bias energy eV . Potential barrier width for electrons occupying the Fermi level is denoted as $\delta_z = z_2 - z_1$. Consider that all the current flowing in the system is due to the tunneling effect.

Probability $D(E_z)$ of the electron transmission through the potential barrier of height $U(z)$ is given by expression (4) in [chapter "Tunneling Effect in Quasiclassical Approximation"](#). For the number of electrons N_1 tunneling through the barrier from electrode 1 into electrode 2, we can write [1], [2]

$$N_1 = \int_{-\infty}^{\infty} \int_{-\infty}^{\infty} \int_{-\infty}^{\infty} \frac{p_z}{4\pi^3 \hbar^3 m} f_1(E)(1 - f_2(E + eV)) D(E_z) dp_x dp_y dp_z =$$

$$= \int_0^{E_m} D(E_z) n(p_z) dE_z \quad (1)$$

where

$$n(p_z) = \frac{1}{4\pi^3 \hbar^3} \int_{-\infty}^{\infty} \int_{-\infty}^{\infty} f_1(E)(1 - f_2(E + eV)) dp_x dp_y \quad (2)$$

and E_m – maximum energy of tunneling electrons.

Integration of expression (2) can be performed in polar coordinates. Because in the model under consideration $p_r^2 = p_x^2 + p_y^2$, $E_r = p_r^2 / 2m$ and total energy is $E = E_z + E_r$, changing variables $p_x = p_r \cos \theta$, $p_y = p_r \sin \theta$, we get

$$\begin{aligned}
n(p_z) &= \frac{1}{4\pi^3\hbar^3} \int_0^{2\pi\infty} \int_0^\infty f_1(E)(1-f_2(E+eV))p_r dp_r d\theta = \\
&= \frac{m}{2\pi^2\hbar^3} \int_0^\infty f_1(E)(1-f_2(E+eV))dE_r
\end{aligned} \tag{3}$$

Substituting (3) in (1), we obtain

$$N_1 = \frac{m}{2\pi^2\hbar^3} \int_0^{E_z} D(E_z)dE_z \int_0^\infty f_1(E_z+E_r)(1-f_2(E_z+E_r+eV))dE_r \tag{4}$$

The number of electrons N_2 tunneling back from electrode 2 into electrode 1 is calculated in the same way. According to (4) from [chapter "Tunneling Effect in Quasiclassical Approximation"](#), the potential barrier transparency in the given case will be such as if positive voltage V is applied to electrode 1 relative to electrode 2. In this case

$$N_2 = \frac{m}{2\pi^2\hbar^3} \int_0^{E_z} D(E_z)dE_z \int_0^\infty f_2(E_z+E_r+eV)(1-f_1(E_z+E_r))dE_r \tag{5}$$

Net electrons flow N through the barrier is obviously $N = N_1 - N_2$. Let us denote

$$\begin{aligned}
\xi_1(E_z) &= \frac{me}{2\pi^2\hbar^3} \int_0^\infty f_1(E)(1-f_2(E+eV))dE_r \\
\xi_2(E_z) &= \frac{me}{2\pi^2\hbar^3} \int_0^\infty f_2(E+eV)(1-f_1(E))dE_r \\
\xi(E_z, eV) &= \xi_1 - \xi_2 = \frac{me}{2\pi^2\hbar^3} \int_0^\infty [f_1(E) - f_2(E+eV)]dE_r
\end{aligned} \tag{6}$$

Then, the tunneling current density J is

$$J = \int_0^{E_\infty} D(E_z)\xi(E_z, eV)dE_z \tag{7}$$

According Fig. 2, $U(z)$ can be written in the form $U(z) = \mu + \varphi(z)$. Then, integrating (4) from [chapter "Tunneling Effect in Quasiclassical Approximation"](#) and using expression (A5) from [Appendix](#), we get

1.2 Tunnel Current in MIM System

$$D(E_z) \propto \exp\left\{-A\delta_z\sqrt{\mu + \bar{\varphi}(z) - E_z}\right\} \tag{8}$$

where $\bar{\varphi}$ – average barrier height relative to Fermi level of the negative electrode; $\bar{\varphi} = \frac{1}{\delta_z} \int_{z_1}^{z_2} \varphi(z)dz$;

$A = 2\beta\sqrt{\frac{2m}{\hbar^2}}$, β – dimensionless factor defined in the [Appendix](#) (A6).

At $T = 0$ K

$$\xi(E_z) = \frac{me}{2\pi^2\hbar^3} \begin{cases} eV, & \text{npu } E_z \in [0; \mu - eV] \\ \mu - E_z, & \text{npu } E_z \in [\mu - eV; \mu] \\ 0, & \text{npu } E_z > \mu \end{cases} \tag{9}$$

Introducing (8) and (9) into (7), we obtain

$$\begin{aligned}
J &= \frac{me}{2\pi^2\hbar^3} \left\{ eV \int_0^{\mu-eV} \exp\left[-A\delta_z\sqrt{\mu + \bar{\varphi} - E_z}\right]dE_z + \right. \\
&\quad \left. + \int_{\mu-eV}^{\mu} (\mu - E_z) \exp\left[-A\delta_z\sqrt{\mu + \bar{\varphi} - E_z}\right]dE_z \right\} \tag{10}
\end{aligned}$$

Integrating (10), we get

$$J = \frac{\alpha}{\delta_z^2} \left\{ \bar{\varphi} \exp\left(-A\delta_z\sqrt{\bar{\varphi}}\right) - (\bar{\varphi} + eV) \exp\left[-A\delta_z\sqrt{\bar{\varphi} + eV}\right] \right\} \tag{11}$$

where $\alpha = e/4\pi^2\beta^2\hbar$.

Thus, expression (11) approximates the tunneling current in the MIM system for arbitrary barrier shape.

Summary

- The general expression (7) to calculate the tunneling current in the MIM system was derived in this chapter.
- The analytic approximate solution (11) of tunneling current in the MIM system was calculated.

References

1. Burshtein E., Lundquist S. Tunneling phenomena in solid bodies. Mir, 1973 (in Russian)
2. John G. Simmons. J. Appl. Phys. - 1963. - V. 34 1793.
3. John G. Simmons. J. Appl. Phys. - 1963. - V. 34 238.

Appendix

Let us integrate an arbitrary function $\sqrt{f(z)}$ from z_1 to z_2 .

$$\int_{z_1}^{z_2} \sqrt{f(z)} dz \quad (A1)$$

Defining \bar{f} as

$$\bar{f} = \frac{1}{\delta_z} \int_{z_1}^{z_2} f(z) dz \quad (A2)$$

where \bar{f} – average value of a function f on the interval from z_1 to z_2 , $\delta_z = z_1 - z_2$. Then equation (A1) can be rewritten as

$$\int_{z_1}^{z_2} \sqrt{f(z)} dz = \sqrt{\bar{f}} \int_{z_1}^{z_2} \sqrt{1 + \frac{[f(z) - \bar{f}]}{\bar{f}}} dz \quad (A3)$$

Considering a Taylor series expansion of the integrand (A3) in and neglecting $[(f(z) - \bar{f})/\bar{f}]^3$ and higher order members, we get

$$\int_{z_1}^{z_2} \sqrt{f(z)} dz = \sqrt{\bar{f}} \int_{z_1}^{z_2} \left\{ 1 + \frac{[f(z) - \bar{f}]}{2\bar{f}} - \frac{[f(z) - \bar{f}]^2}{8\bar{f}^2} \right\} dz \quad (A4)$$

The second term in (A4) vanishes upon integration, therefore (A4) can be expressed as

$$\int_{z_1}^{z_2} \sqrt{f(z)} dz = \beta \sqrt{\bar{f}} \delta_z \quad (A5)$$

where the correction factor is

$$\beta = 1 - \frac{1}{8\bar{f}^2 \delta_z} \int_{z_1}^{z_2} [f(z) - \bar{f}]^2 dz \quad (A6)$$

John G. Simmons Formula in a Case of Small, Intermediate and High Voltage (Field Emission Mode)

According chapter [John G. Simmons Formula](#), the approximate expression for the tunneling current in the MIM system can be written as [1]:

$$J = \frac{\alpha}{\delta_z^2} \left\{ \bar{\phi} \exp(-A \delta_z \sqrt{\bar{\phi}}) - (\bar{\phi} + eV) \exp[-A \delta_z \sqrt{\bar{\phi} + eV}] \right\} \quad (1)$$

where $\alpha = e/4\pi^2 \beta^2 \hbar$, $A = 2\beta \sqrt{\frac{2m}{\hbar^2}}$, $\bar{\phi}$ – average barrier height, δ_z – barrier width, V – voltage between electrodes.

Small voltage

At low voltages $\bar{\phi} \gg eV$, expression (1) can be simplified [1]

$$J = \frac{\gamma \sqrt{\bar{\phi}} V}{\delta_z} \exp(-A \delta_z \sqrt{\bar{\phi}}) \quad (2)$$

where $\gamma = \frac{e\sqrt{2m}}{4\beta\pi^2 \hbar^2}$. Since $\bar{\phi} \gg eV$, we can consider that $\bar{\phi}$ doesn't depend on V . Thus, in the case of small applied voltage, the tunneling current proportionate to V . Energy diagram of the MIM system then $\bar{\phi} \gg eV$ is shown on Fig. 1.

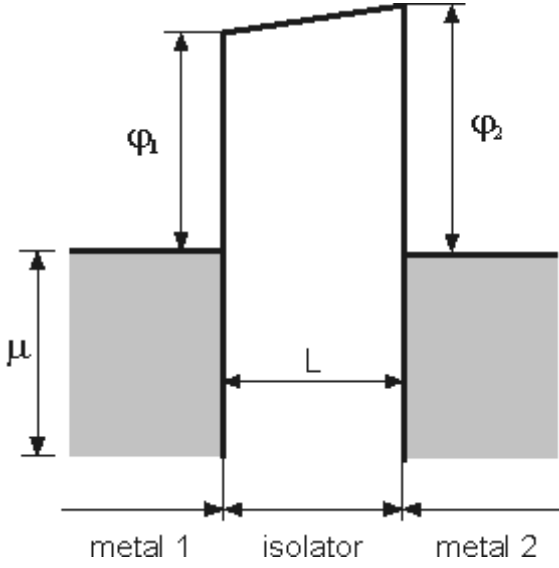


Fig. 1. Potential barrier in the MIM system then $V \sim 0$.
 ϕ_1 and ϕ_2 – work function of the left and right metals,
 respectively

In this case, as shown on Fig. 1, $\delta_z = L$ and $\bar{\phi} = (\phi_1 + \phi_2)/2$

Intermediate voltage

If $eV < \phi_2$, then $\delta_z = L$ and $\bar{\phi} = (\phi_1 + \phi_2 - eV)/2$ (Fig. 2).

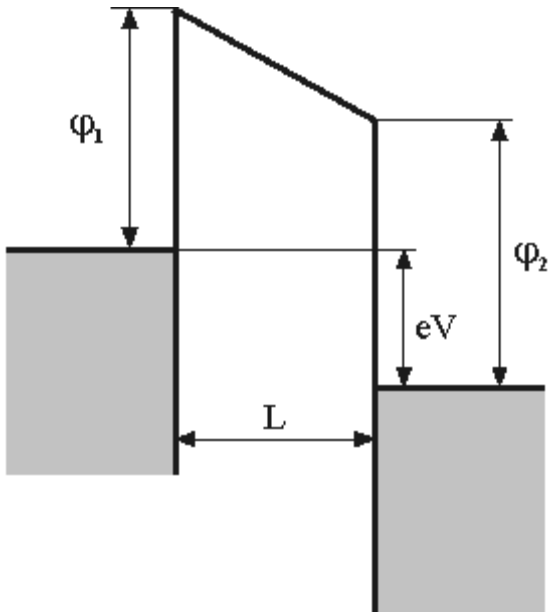


Fig. 2. Potential barrier in the MIM system then $eV < \phi_2$.
 ϕ_1 and ϕ_2 – work function of the left and right metals,
 respectively

In [2] it is shown, that for this case the tunneling current-voltage relation is given by

$$J = \frac{\gamma \sqrt{\bar{\phi}}}{\delta_z} \exp(-A \delta_z \sqrt{\bar{\phi}}) (V + \sigma V^3) \quad (3)$$

$$\text{where } \sigma = \frac{(Ae)^2}{96 \bar{\phi} \delta_z^2} - \frac{Ae^2}{32 \delta_z \bar{\phi}^{3/2}}$$

High voltage – Field emission mode

The case when $eV > \phi_2$ corresponds to energy diagram shown in **Fig. 3** and to the following $\delta_z = L \phi_1 / (\phi_1 - \phi_2 + eV)$, $\bar{\phi} = \phi_1 / 2$.

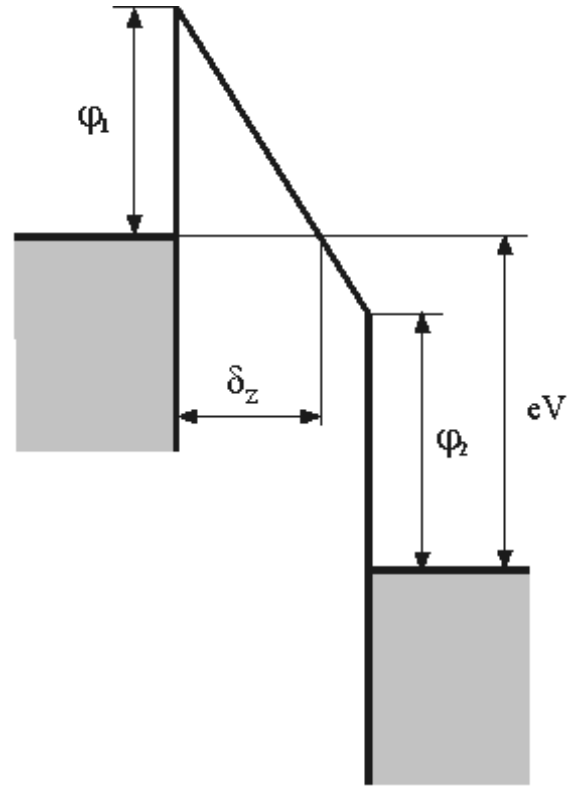


Fig. 3. Potential barrier in the MIM system then $eV > \phi_2$.
 ϕ_1 and ϕ_2 – work function of the left and right metals,
 respectively.

Substituting δ_z and $\bar{\phi}$ into equation (1), we obtain

$$J = \frac{e^3 F^2}{8\pi^2 \hbar \phi_1 \beta^2} \left\{ \exp \left[-\frac{2\beta}{eF} \phi_1^{3/2} \frac{\sqrt{2m}}{\hbar} \right] - \left(1 + \frac{2eV}{\phi_1} \right) \exp \left[-\frac{2\beta}{eF} \phi_1^{3/2} \frac{\sqrt{2m}}{\hbar} \sqrt{1 + \frac{2eV}{\phi_1}} \right] \right\} \quad (4)$$

where $F = V/L$ – electric field strength.

At high applied voltage ($eV > \phi_1 + \mu$) the Fermi level of electrode 2 is lower than the conduction band bottom of electrode 1. Under such conditions, electrons can not tunnel from electrode 2 into electrode 1 because of lack of empty states. An inverse situation is for electrons tunneling from electrode 1 into empty states of electrode 2. This process is similar to autoelectronic emission from a metal into vacuum. Thus, since $eV > \phi_1 + \mu$, the second summand in (4) can be neglected and for the current we get

$$J = \frac{e^3}{8\pi^2 \hbar \beta^2} \frac{F^2}{\phi_1} \exp \left[-\frac{2\beta}{e} \frac{\sqrt{2m}}{\hbar} \frac{\phi_1^{3/2}}{F} \right] \quad (5)$$

where coefficient $\beta = 23/24$. This result agrees qualitatively with an analytical expression for the field emission current density [3].

Thus, using formulas (2)–(5), we can compute the tunnel current at given system parameters and plot current-voltage characteristics. Fig. 4 shows theoretical tunneling current-applied voltage plot in case of carbon electrode 1 ($\phi_1 = 4,7$ eV) and platinum electrode 2 ($\phi_2 = 5,3$ eV) at $\delta_z = 5$ Å and contact area $S = 10^{-17}$ m².

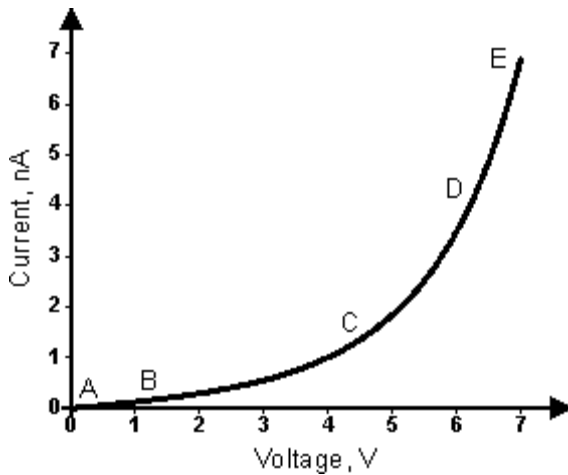


Fig. 4. Current-voltage characteristic for carbon electrode 1 and platinum electrode 2 at $\delta_z = 5$ Å and contact area 10^{-17} m².

Parts of $J(V)$ curve correspond to the following expressions:
AB – (22), BC – (23), CD – (24), DE – (25).

Summary

- Depend upon magnitude of applied voltage, formula (1) can be simplified (2)–(5).
- It is possible to describe the experimental tunneling current dependences by approximated expressions (2)–(5) in accordance with magnitude of applied voltage.

References

1. John G. Simmons. J. Appl. Phys. - 1963. - V. 34 1793.
2. John G. Simmons. J. Appl. Phys. - 1963. - V. 34 238.
3. Dobretzov L.N., Gomounova M.V. Emission electronics. Nauka, 1966 (in Russian)

CONTACT DETAILS

Building 167, Zelenograd, 124460, Moscow, Russia
Tel: +7(095)535-0305, 913-5736
Fax: +7(095) 535-6410, 913-5739

e-mail: spm@ntmdt.ru; <http://www.ntmdt.ru>

"Observed" Physical Quantities in STM

Current-Voltage Characteristic

Measurement of relation between tunneling current and probe-sample voltage is carried out in $J(V)$ spectroscopy mode. The $J(V)$ spectroscopy is based on the dependence of tunneling current on number of electron states N , forming a tunneling contact of conductors, in the energy range from the Fermi level μ to $\mu - eV$ (Fig. 1), which at $T = 0$ gives (see (7) in [chapter "John G. Simmons Formula"](#))

$$J \propto N = \int_{\mu - eV}^{\mu} \xi(E_z) dE_z \quad (1)$$

Thus the tunneling current dependence $J(V)$ at constant tip-sample separation δ_z represents an allocation of torn bonds as well as other electron states corresponding different energies, i.e. energy band structure of either tip or surface. Function $\xi(E_z)$, which was introduced in (6) of [chapter "John G. Simmons Formula"](#), depends on electron state density of phase space plane which is normal to tunneling direction at given E_z .

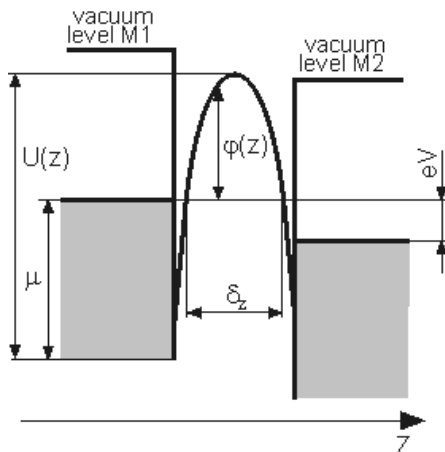


Fig. 1. Model of MIM system with an arbitrary shape potential barrier. Positive potential is applied to the right metal

Using expression (1) and $J(V)$ curve at constant tip-sample separation δ_z , it is possible to compute the density of electronic states:

$$\frac{dJ}{d(eV)} \propto \xi(\mu - eV) \quad (2)$$

Thus, inspection of $J(V)$ and its derivative $dJ/d(eV)$ curves allows to investigate energy levels distribution with atomic resolution. It is possible to determine a conductivity type, in particular for semiconductors – to detect the valence band, conductivity band and impurity band. [1]–[3].

According to (2) and (3) from [chapter "John G. Simmons Formula in a Case of Small, Intermediate and High Voltage \(Field Emission Mode\)"](#) tunneling conductivity $G = dJ/dV$ does not depend on applied voltage V in case $eV \ll \bar{\phi}$.

$$G = \frac{\gamma \sqrt{\bar{\phi}}}{\delta_z} \exp\left(-A \delta_z \sqrt{\bar{\phi}}\right) \quad (3)$$

at $eV < \phi_2$ relation between G and V is parabolic

$$G \approx \gamma \sqrt{\bar{\phi}} \exp\left(-A \sqrt{\bar{\phi}}\right) (1 + 3\sigma V^2) \quad (4)$$

On Fig. 2, 3 experimental dependences $J(V)$, $G(V)$, which were measured for Pt and HOPG samples and Pt-Ro probe using STM Solver P47, is shown. Experimental data are in good agreement with the theoretical predictions (1)–(4).

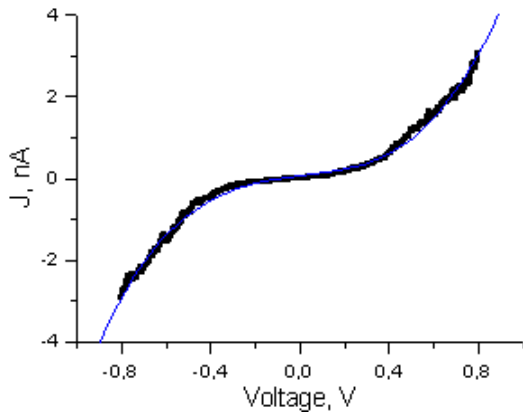


Fig. 1a. Experimental (points) and theoretical (solid line) dependences $J(V)$ for Pt

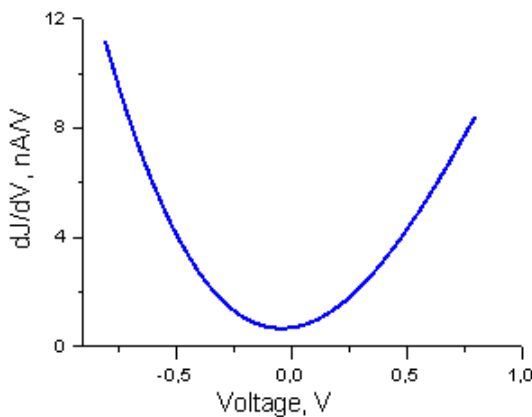


Fig. 1b. Experimental dependence $G(V)$ for Pt

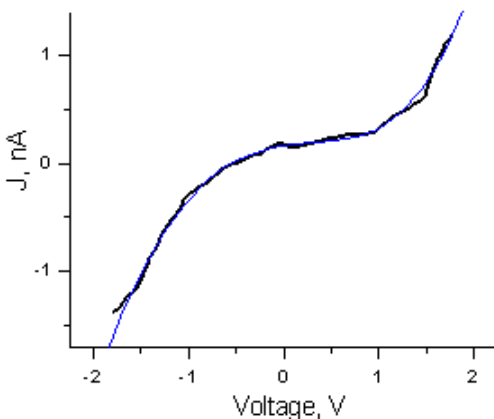


Fig. 2a. Experimental (points) and theoretical (solid line) dependences $J(V)$ for HOPG

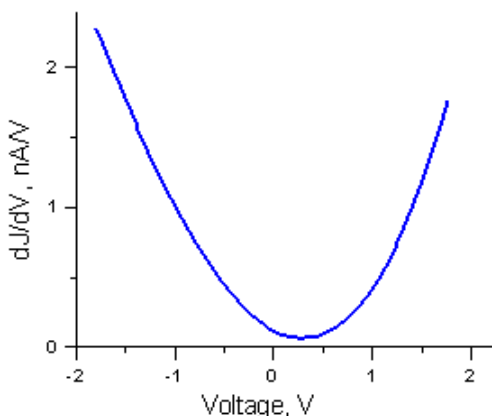


Fig. 2b. Experimental dependence $G(V)$ for HOPG

Summary

- Tunneling current-voltage characteristic represents number of electron states and their distribution in energy spectrum of electrodes which creates tunneling contact.
- Differential conductance G is proportional an electron state density. For metals at low voltages G does not depend on applied voltage (3). At intermediate voltages the relation between G and applied voltage is parabolic (4).
- Experimental current-voltage and differential characteristic are in good agreement with theory.

References

1. G. Binnig., H. Rohrer. Scanning tunneling microscopy. *Helv. Phys. Acta.* - 1982, - V. 55 726.
2. A. Burshtein, S. Lundquist. Tunneling phenomena in solid bodies. Mir, 1973 (in Russian).
3. E. Wolf. Electron tunneling spectroscopy principles. Kiev: "Naukova Dumka", 1990, 454 p. (in Russian).

Current-Distance Characteristic

Measurement of relation between tunneling current and tip-sample distance is carried out in $I(\delta_z)$ spectroscopy mode. According to (11) from [chapter "John G. Simmons Formula"](#), in absence of a condensate, a typical current-height relation is an exponential current decay (Fig. 1) with a characteristic length of a few angstrom [1], [2].

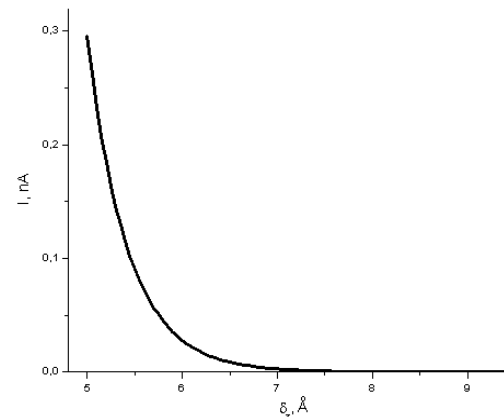


Fig. 1. Theretical $I(\delta_z)$ curve for Pt sample and Pt-Ro probe

Inspecting an experimental $I(\delta_z)$ curve, it is possible to estimate the potential barrier height $\bar{\phi}$. If tip-sample bias V is small enough, then

according to [chapter "John G. Simmons Formula in a Case of Small, Intermediate and High Voltage \(Field Emission Mode\)"](#), tunneling current can be written as

$$I = \frac{\gamma S \sqrt{\bar{\phi}} V}{\delta_z} \exp(-A \delta_z \sqrt{\bar{\phi}}) \quad (1)$$

where $\gamma = \frac{e\sqrt{2m}}{4\beta\pi^2\hbar^2}$, $A = 2\beta\sqrt{\frac{2m}{\hbar^2}}$, S – contact area, m – free electron mass, e – elementary charge, \hbar – Planck's constant.

From (1) $\bar{\phi}$ can be expressed through some analytical function of $d \ln(I)/d\delta_z$. Finding the natural logarithm of (1) and differentiate the result by δ_z one can obtain

$$\frac{d \ln(I)}{d\delta_z} = -\frac{1}{\delta_z} - A\sqrt{\bar{\phi}} \quad (2)$$

If $\delta_z \gg 1/A\sqrt{\bar{\phi}}$, then $\bar{\phi}$ can be expressed from (2) by following way

$$\bar{\phi} = \frac{1}{A^2} \left(\frac{d \ln(I)}{d\delta_z} \right)^2 \approx 10^{-20} \left(\frac{d \ln(I)}{d\delta_z} \right)^2 \text{ eV} \quad (3)$$

where $d \ln(I)/d\delta_z$ is expressed in m^{-1} .

Emphasize, that in most cases the condition $\delta_z \gg 1/A\sqrt{\bar{\phi}}$ realizes practically always. For instance, if $\bar{\phi} = 4 \text{ eV}$, then expression (3) will be correct at $\delta_z \gg 0,5 \text{ \AA}$.

Experimental $I(\delta_z)$ curve for Pt-flim which was measured using Pt-Ro probe in STM (Solver P47) on air, is shown on Fig. 2.

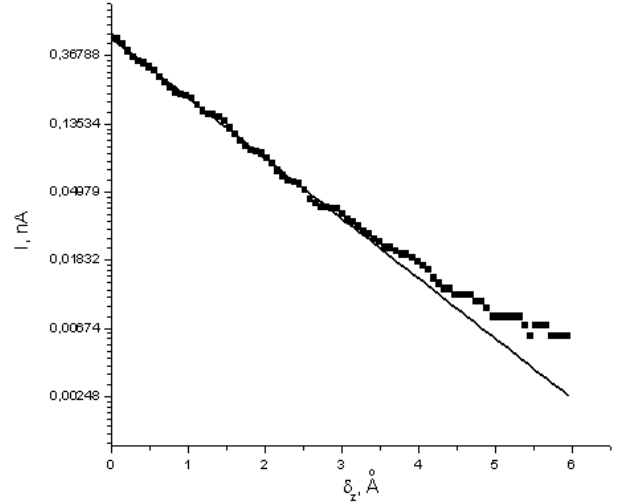


Fig. 2. Experimental $I(\delta_z)$ curve (semilogarithmic scale).
Solid line – approximation $I = 0,47 \exp(-10\delta_z/11)$.

Substituting value of approximated straight line slope $d \ln(I)/d\delta_z = -0,09 \text{ nm}^{-1}$ in (3), we obtain, that $\bar{\phi} \approx 0,8 \text{ eV}$. Theoretical value of $\bar{\phi}$, in case, then both electrodes are produced from Pt, equals $\bar{\phi} = 5,3 \text{ eV}$. Thus, experimental value of $\bar{\phi}$ is lower by a factor about 6 than theoretical one. Most probably, the main reason of this difference is condensate presence on electrodes surface. Even for fresh surfaces of pyrolytic graphite at maximum $d \ln(I)/d\delta_z$ values, the corresponding values of $\bar{\phi}$ are less than several tenths of eV. These values are deliberately less than those known from high vacuum and low temperature STM experiments for the same samples and tips [3]. Values of $\bar{\phi}$ derived from experiments in air are close to those obtained using STM configured for electrochemical measurements *in situ* when liquid polar medium exists between sample and tip [3]. A condensate in the STM operating in air is evidently the analogue of such a medium. Thus, the condensate occurrence on the sample surface results in the STM image quality deterioration and values of $\bar{\phi}$ understatement.

Frequently $I(\delta_z)$ spectroscopy is used for a determination of tip quality (sharpness).

Experimental $I(\delta_z)$ curves, which are measured at investigation of HOPG surface using "good" and "poor" sharp tip of Pt-Ro probe, is shown on Fig. 3, 4.

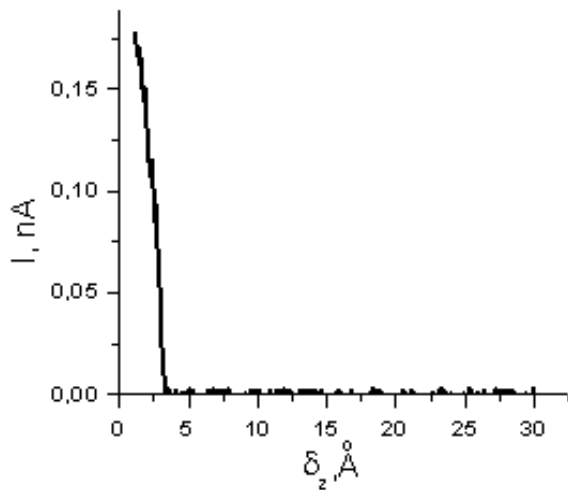


Fig. 3. $I(\delta_z)$ spectroscopy for a "good-shape" STM tip

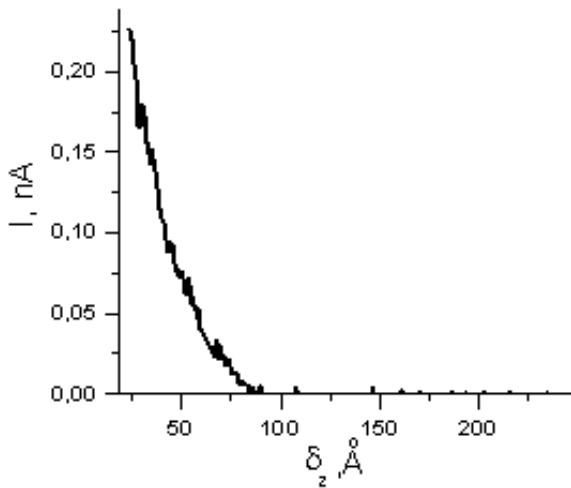


Fig. 4. $I(\delta_z)$ spectroscopy for a "poor-shape" STM tip

Tip quality criterion is following: 1) if tunneling current drops twice at tip-sample distance less than 3 Å, then tip quality is very good; 2) if this distance is about 10 Å, then atomic resolution can be still obtained on HOPG using such STM tip; 3) if the current drops at distance equals or more than 20 Å, then this STM tip should be replaced or sharpened [4].

Summary

- It is possible to estimate electron work-function of investigated material using $I(\delta_z)$ spectroscopy (3).
- The difference between experimental and table values of work-function is connected with the condensate presence on electrodes surface.
- In practice $I(\delta_z)$ curve is used for a determination of STM tip quality (sharpness).

Reference

1. John G. Simmons. J. Appl. Phys. – 1963. – V. 34 1793.
2. G. Binnig., H. Rohrer. Helv. Phys. Acta. – 1982, – V. 55 726.
3. S. Yu. Vasilev, A. V. Denisov. Journal of technical physics. – 2000, – vol. 70, num. 1 (in Russian).
4. NT-MDT. Solver P47 users guide.

Measurements of the Electronic States Density

In chapter [Current-Voltage Characteristic](#) we considered the spectroscopy of electronic states. Meanwhile, at given eV it is possible to measure the electronic states distribution across the sample surface.

The electronic states density distribution measurement is performed in parallel with surface topography imaging in the $J = const$ mode. Instead of constant tip bias V_0 , the alternating voltage $V = V_0 + b \sin \omega t$ is applied between sample and tip, where $b \sin \omega t$ – the alternating signal having amplitude $b \ll V_0$ (Fig. 1). Then, the net tunneling current is proportional to the following

$$J \propto N_0 + N_{\sim} \quad (1)$$

$$\text{where } N_0 = \int_{\mu - eV_0}^{\mu} \xi(E_z) dE_z$$

$$\text{and } N_{\sim} = \xi(\mu - eV_0) e b \sin \omega t.$$

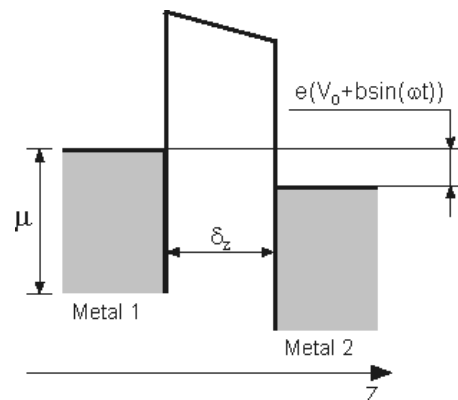


Fig. 1. Diagram of MIM system, when applied voltage is modulated as $V = V_0 + b \sin \omega t$

Thus, the total current flowing through the tunneling gap is equal to $J = J_0 + J_{\sim}$, where J_{\sim} – alternating component. Because J_0 is held constant during the scan and $eb = \text{const}$, the alternating tunneling current amplitude is proportional to the electronic states density $\xi(\mu - eV_0)$. Hence, measuring the alternating current amplitude during scan allows for the mapping of the electronic states density in standard units. Since $b \ll V_0$, then J_{\sim}/b is actually dJ/dV .

The frequency ω , as mentioned above, should be much more than the reciprocal feedback integrator time constant and be limited by maximum permissible scan frequency.

Summary

- Modulation of applied voltage V results in oscillations of tunneling current J . Amplitude of such oscillations depends on electron properties of electrodes, which create a tunneling contact.
- Using this method, it is possible to measure distribution of electron state density on investigated sample surface.

References

1. G. Binnig, H. Rohrer. Helv. Phys. Acta. – 1982, – V. 55 726.
2. A. Burshtein, S. Lundquist. Tunneling phenomena in solid bodies. Mir, 1973 (in Russian).
3. E. Wolf. Electron tunneling spectroscopy principles. Kiev: "Naukova Dumka", 1990, 454 p. (in Russian).

Work-Function Distribution Study

In chapter [Current-Distance Characteristic](#) we considered that it is possible to estimate average electron work-function of electrodes using current-distance experimental curves. However, these measurements give work-function values only in small region where one electrode is located over another. In STM there is another method which is able to measure distribution of work-function along all investigated sample surface.

The work function distribution measurement is performed in parallel with surface topography imaging in the $J = \text{const}$ mode. In this case, the Z-axis piezo tube motion is determined not only by the feedback signal but also by application of an alternating signal producing motion law $\Delta Z = a \cos(\omega t)$. Accordingly, the tip-sample separation is $\delta_z = \delta_{z0} + a \cos(\omega t)$, where parameter being $a \ll \delta_{z0}$, δ_{z0} – tip-sample separation held constant through the feedback, ω – Z-axis piezo tube resonant frequency (Fig. 1).

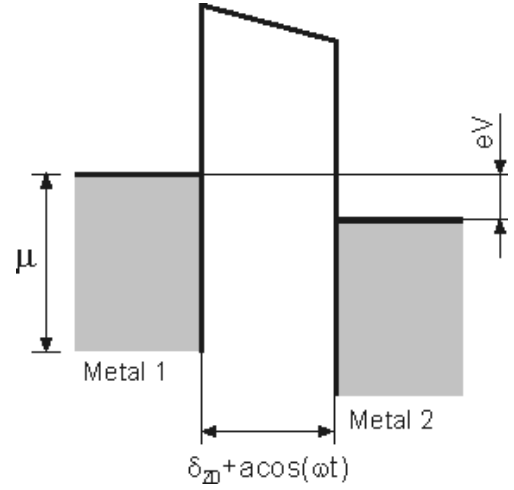


Fig. 1. Diagram of MIM system when tip-sample distance is modulated as $\delta_z = \delta_{z0} + a \cos(\omega t)$

If voltage applied between tip and sample is small $V \approx 0$, then according to designations introduced, expression (2) from [chapter 1.2.2](#) can be transformed to the following

$$J = \frac{\gamma \sqrt{\phi} V}{\delta_{z0} + a \cos(\omega t)} \exp\left(-A \sqrt{\phi} (\delta_{z0} + a \cos(\omega t))\right) \approx J_0 \left[1 - A \sqrt{\phi} a \cos(\omega t)\right] \quad (1)$$

where $J_0 = J(\delta_{z0})$.

Thus, total current flowing through the tunneling gap in this case is equal to $J = J_0 + J_{\sim}$, where J_{\sim} – alternating tunneling current. Because J_0 is held constant during the scan, the alternating tunneling current amplitude is proportional to the square root of the tip and the sample work function half-sum. Assuming that tip work function is constant during

scanning, the J_{\sim} amplitude will depend only on the studied surface work function.

The frequency ω , as mentioned above, should be much more than the reciprocal feedback integrator time constant and be limited by maximum permissible scan frequency.

■ Summary

- Modulation of tip-sample distance results in oscillations of tunneling current J .
- Using this method it is possible to measure the distribution of work-function along all investigated sample surface.

■ References

1. G. Binnig., H. Rohrer. Scanning tunneling microscopy. Helv. Phys. Acta. - 1982, - V. 55 726.
2. A. Burshtein, S. Lundquist. Tunneling phenomena in solid bodies. Mir, 1973 (in Russian).
3. E. Wolf. Electron tunneling spectroscopy principles. Kiev: "Naukova Dumka", 1990, 454 p. (in Russian).

CONTACT DETAILS

Building 167, Zelenograd, 124460, Moscow, Russia
Tel: +7(095)535-0305, 913-5736
Fax: +7(095) 535-6410, 913-5739

e-mail: spm@ntmdt.ru; <http://www.ntmdt.ru>